

Fig. 2 Schematic diagram of experimental apparatus [8]

### III. RESULTS AND DISCUSSION

In the author's previous report [8], he found that the flow of pulp suspensions in a square duct can be classified into five patterns from the viewpoint of the pulp fiber behavior, as shown schematically in Fig. 3.

In Fig. 4, we first show an example of results for the pressure loss at several fiber concentrations in a circular pipe. The relation between the pressure loss and mean fluid velocity appears to form a similar curve for different concentrations, although different pipe diameters and raw materials of the pulp were used in previous experiments [1]–[4]. Unfortunately, there are still many unknown points with regard to the problem that such flow behaviors appear under what conditions [9]. To survey these points, it is essential to appropriately define the strength of fiber networks and then to find the flow field at which the formed flocks disperse. For the disruption of flocks, it is necessary that the shear stress in a flow field is greater than the strength of the fiber networks. We can consider the yield shear stress as a useful index for evaluating the strength of fiber networks. In the following, with the above viewpoint, we will discuss the flow characteristics shown in the  $\Delta P/L - U_a$  curve in Fig. 1.

The fibers flowing in pipes are not distributed uniformly as shown in Fig. 3. Therefore, the relation between the shear stress and the shear rate of a pulp suspension flow is different from that for a homogeneous Newtonian fluid. Fig. 5 shows the viscosity  $\mu_w$  at the pipe wall versus the mean velocity  $U_a$  in the pipe of  $d=22\text{mm}$ . The broken lines in Fig. 5 show where the flow pattern of  $C_s=0.8\%$  divides. Approximating the experimentally obtained velocity distribution by  $u=u(r)$ , we calculate the viscosity  $\mu_w$  as

$$\mu_w = \tau / (-du/dr)_{r=a} \quad (1)$$

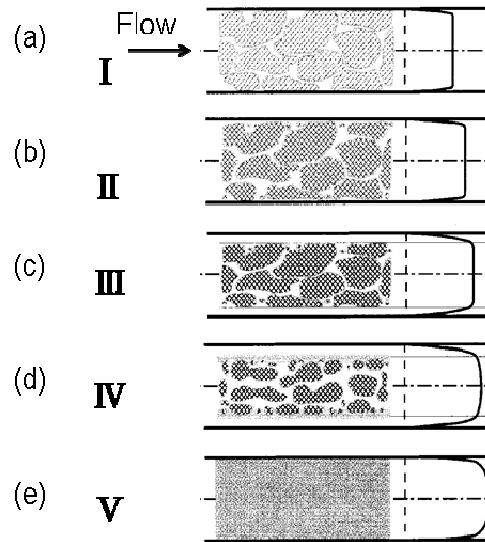
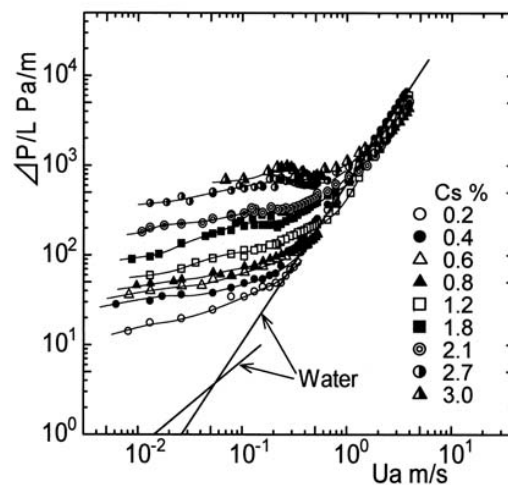


Fig. 3 Typical flow patterns of pulp suspensions [8] (a) Pattern I: Plug flow with strong interaction between fiber and pipe wall. (b) Pattern II: Plug flow with hydrodynamic shear and fiber-wall interaction. (c) Pattern III: Plug flow with water annulus in laminar shear. (d) Pattern IV: Mixed flow with fiber/water annulus and transitional flow from laminar to turbulent. (e) Pattern V: Turbulent flow with distributed pulp fibers

Fig. 4 Pressure loss for several fiber concentrations for  $d=22\text{ mm}$ .

The viscosity  $\mu_w$  at the pipe wall is larger than that for water. It increases as the fiber concentration increases. Nevertheless, in the laminar flow of patterns I to III, the viscosity decreases with increasing  $U_a$ .

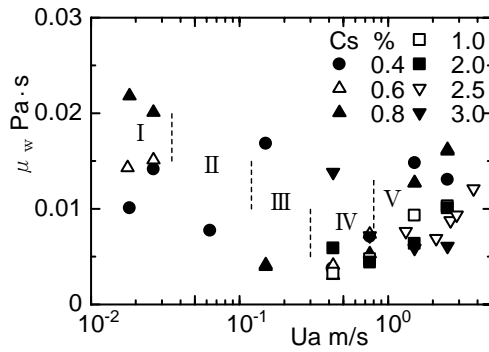


Fig. 5 Relationship between viscosity  $\mu_w$  at pipe wall and mean velocity  $U_a$

#### A. Flow Properties at Low Velocity (Patterns I and II)

The pulp suspension possesses so-called yield shear stress. This implies that a pressure gradient exceeding a certain magnitude is necessary for pulp suspensions to keep flowing. The  $\Delta P/L-U_a$  curves in Fig. 4 are those for which the flowing state is maintained. The yield shear stress  $\tau_0$  is obtained from the pressure loss when an intermittent flow occurs at a low velocity. The results are shown in Fig. 6. In Fig. 6, we show the results for the wall shear stresses,  $\tau_c$  and  $\tau_t$ , as described later. Here,  $\tau_c$  denotes the wall shear stress at which the transition to turbulent flow occurs, and  $\tau_t$  is that when the flow state can be considered to be turbulent over the whole cross section. From Fig. 6, the yield shear stress  $\tau_0$  can be roughly expressed using only the fiber concentration  $C_s$  as

$$\tau_0 = 0.28 C_s^{1.6} \quad (2)$$

( $\tau_0$ : Pa, valid for  $d=10-40$  mm and  $C_s=0.3-3\%$ ).

Expression (2) is a well-known empirical equation [11]. A dependence of  $\tau_0$  on the pipe diameter  $d$  cannot be clearly recognized.

In pattern I, the pulp fibers become a massive flock and move as a rigid body, as shown in Fig. 3 (a). A dynamic frictional force corresponding to the yield shear stress is generated between the pulp fibers and pipe wall. When the flow rate is slightly increased, the flow pattern changes to type II. A very thin water layer begins to form annularly on the pipe wall as shown in Fig. 3 (b). Therefore, both the dynamic frictional force of the massive pulp fibers and the viscous force of the water layer act on the pipe wall simultaneously. Thereby, the pressure loss increases in proportion to  $U_a$ . Such behavior of pulp suspensions at a low velocity exhibits the Bingham property. In pattern II, the dynamic frictional force of the massive pulp fibers acting on the wall is softened as the water annulus is formed. Thus, the viscosity  $\mu_w$  at the pipe wall becomes small compared with that of pattern I (see Fig. 5).

#### B. Flow Properties at Moderate Velocity (Pattern III)

For pattern III, the suspensions are two-phase systems in which the flowing fluid consists of a thin water annulus layer

and a plug flow in the central part of the cross section. Then the flocks of pulp fibers are forced into the plug flow region as the velocity  $U_a$  increases. This causes the water annulus to become thicker, as illustrated in Fig. 3 (c). Therefore, the changes in the shear rate  $\dot{\gamma}_w$  at the wall are less variable when  $U_a$  increases and  $\mu_w$  takes a minimum value relative to  $U_a$  as shown in Fig. 5. That is, in the laminar flow for patterns I to III, the shear-thinning character can be recognized in the pulp suspensions in the vicinity of the pipe wall.

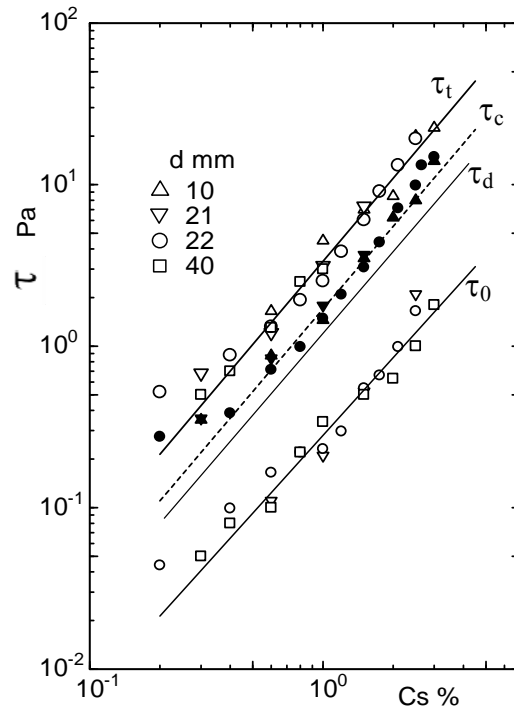


Fig. 6 Relationship between wall shear stress  $\tau$  and fiber concentration  $C_s$ .  $\tau_0$ : yield shear stress,  $\tau_d$ : disruptive shear stress,  $\tau_c$ : critical shear stress,  $\tau_t$ : turbulent shear stress

In pattern III, the wall shear stress  $\tau_{III}$  is roughly expressed as

$$\tau_{III} \approx (0.46 - 1.1) C_s^{1.7} \quad (3)$$

( $\tau_{III}$ : Pa, valid for  $C_s=0.4-3\%$  and  $d=10-40$  mm).

The above expression is not dependent on the pipe diameter as in the case of  $\tau_0$ .

#### C. Flow Properties at High Velocity (Patterns IV and V)

In pattern III, when the fluid velocity increases, the fiber concentration in the plug region also increases and the fibers there become more compressed. As a result, the thickness of the water annulus cannot increase further and a higher shear flow in the water annulus ensues. Thus, the network of flocculated pulp fibers close to the water layer starts to disintegrate (pattern IV). As a result,  $\mu_w$  at the pipe wall increases as shown in Fig. 5. Nevertheless, the shear stress  $\tau_{IV}$  at the wall does not change

significantly and takes a value of  $\tau_{IV} \approx 1.1C_s^{1.7}$ . From these findings, we can conclude that the flocculated pulp fibers begin to disentangle when the shear stress  $\tau_d$  is about four times the yield shear stress  $\tau_0$ . The dot-dashed line in Fig. 6 indicates the disruptive shear stress  $\tau_d$ .

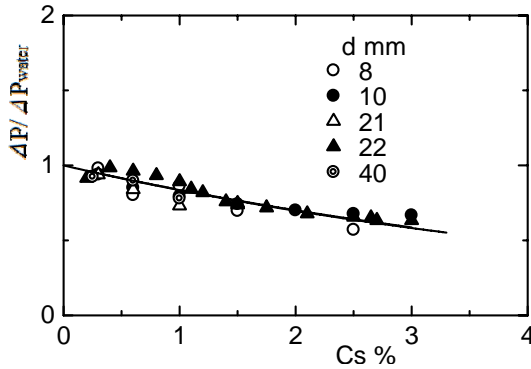


Fig. 7 Effect of fiber concentration on pressure loss in turbulent flow

With a further increase in the flow rate, turbulence occurs in the pulp suspensions and the fluid undergoes a transition from laminar to turbulent flow. Consequently, the pressure loss rapidly increases as  $U_a$  increases. The critical velocity is indicated as  $P_c$  in Fig. 1. The transition can be considered to start when the shear stress in the water layer exceeds a certain value. The experimental values of the critical shear stress  $\tau_c$  at the pipe wall are expressed by the broken line in Fig. 6. That is,

$$\tau_c \approx 1.7C_s^{1.7} \quad (4)$$

( $\tau_c$ : Pa, valid for  $C_s=0.4-3\%$  and  $d=10-40$  mm).

$\tau_c$  increases exponentially with  $C_s$ , similar to (2).

With a further increase in the flow rate, the pulp suspensions become turbulent over the whole cross section, and the turbulent stresses increase to disrupt the fiber networks of the plug. The flow pattern changes to type V, and the corresponding flow velocity is denoted by  $P_t$  in Fig. 1. In this regime,  $\mu_w$  is the turbulent viscosity, which rapidly increases with  $U_a$  as shown in Fig. 6. The wall shear stress  $\tau_t$  at which the flow can be considered to be thoroughly turbulent in the pipe is expressed as

$$\tau_t \approx 3.3C_s^{1.7} \quad (5)$$

( $\tau_t$ : Pa, valid for  $C_s=0.4-3\%$  and  $d=10-40$  mm)

The turbulent shear stress  $\tau_t$  is at least ten times the yield shear stress  $\tau_0$ , and the pulp fibers are dispersed almost uniformly in the pipe.

For flows in pattern V, the pressure loss  $\Delta P$  is smaller than that for water, and the decrease in  $\Delta P$  becomes large as  $C_s$  increases as shown in Fig. 4. Thus, we compare it with that for

the water in the turbulent flow region (pattern V). The results are given in Fig. 7. The pressure loss ratio can be expressed approximately as

$$\Delta P/\Delta P_{water} = \exp(-0.18C_s) \quad (C_s: \%). \quad (6)$$

The above expression is also unrelated to the pipe diameter  $d$ .

#### IV. CONCLUSIONS

The flow characteristics for five regimes were examined one by one. The principal findings of this study are summarized as follows.

- (1) The pulp suspensions have the properties of a Bingham fluid. The yield shear stress  $\tau_0$  at the pipe wall increases with increasing fiber concentration and does not depend on the pipe diameter.  $\tau_0$  can be expressed by the experimental equation (2).
- (2) The flocks of the pulp fibers become disrupted by the shear stress  $\tau_d$  when it exceeds about four times the yield shear stress  $\tau_0$ . When the wall shear stress becomes about ten times larger than the yield shear stress  $\tau_0$ , the pulp suspension is dispersed uniformly over the pipe cross section.
- (3) The pressure loss in a turbulent flow becomes smaller than that for water with increasing fiber concentration. The rate of reduction can be approximately expressed by (5).

#### ACKNOWLEDGMENT

The author would like to thank Mr. Taro Fujimoto of MHI Solution Technologies Co., Ltd., for useful discussions and Mr. Kazuhiro Echizen of Oji Paper Co., Ltd., for providing the pulp suspensions. This work was supported in part by MEXT KAKENHI (23560212).

#### REFERENCES

- [1] A. A. Robertson and S. G. Mason, "Flocculation in flowing pulp suspensions," *Pulp and Paper Magazine of Canada*, Convention Issue (1954), pp. 263-269.
- [2] A. A. Robertson and S. G. Mason, "The flow characteristics of dilute fiber suspensions," *TAPPI*, Vol. 40, No. 5 (1957), pp. 326-334.
- [3] O. L. Forgacs, A. A. Robertson and S. G. Mason, "The hydrodynamic behaviour of paper-making fibers," *Pulp and Paper Magazine of Canada*, Vol. 59 (1958), pp. 117-128.
- [4] G. G. Duffy, A. L. Titchener, P. F. W. Lee and K. Moller, "The mechanisms of flow of pulp suspensions in pipes," *Appita*, Vol. 29, No.5 (1976), pp. 363-370.
- [5] R. Whalley and M. Ebrahimi, "Optimum control of a paper making machine headbox," *Applied Mathematical Modelling*, Vol. 26 (2002), pp. 665-679.
- [6] M. Linnala, H. Ruotsalainen, E. Madetoja, J. Savolainen and J. Hämäläinen, "Dynamic simulation and optimization of an SC papermaking line – illustrated with case studies," *Nordic Pulp and Paper Research Journal*, Vol. 25, No. 2 (2010), pp. 213-220.
- [7] J. Hämäläinen, E. Madetoja and H. Ruotsalainen, "Simulation-based optimization and decision support for conflicting objectives in papermaking," *Nordic Pulp and Paper Research Journal*, Vol. 25, No. 3 (2010), pp. 405-410.
- [8] M. Sumida, "Flow characteristics of pulp liquid in straight ducts," *Engineering and Technology*, Issue 74 (2013).
- [9] H. Cui and J. R. Grace, "Flow of pulp fibre suspension and slurries: A review," *Int. J. Multiphase Flow*, Vol. 33 (2007), pp. 921-934.

- [10] M. Sumida, "Development of a technique for measuring fiber concentration of pulp liquid flow," *Fluid Dynamics and Thermodynamics Technologies*, Vol. 33 (2012), pp. 118-124.
- [11] C. P. J. Bennington, "The yield stress of fibre suspensions," *Canadian Journal of Chemical Engineering*, Vol. 68 (1990), pp. 748-757.